Molecular Biology of the Cell
Vol. 11, 481–495, February 2000

Role for Dynamin in Late Endosome Dynamics and Trafficking of the Cation-independent Mannose 6-Phosphate Receptor

Paolo Nicoziani,*† Frederik Vilhardt,* Alicia Llorente,‡ Leila Hilout,§ Pierre J. Courtoy,§ Kirsten Sandvig,‡ and Bo van Deurs*‖

*Structural Cell Biology Unit, Department of Medical Anatomy, The Panum Institute, University of Copenhagen, DK-2200 Copenhagen, Denmark; ‡Institute for Cancer Research, The Norwegian Radium Hospital, Montebello, 0310 Oslo, Norway; and §Unite de Biologie Cellulaire, Christian de Duve Institute of Cellular Pathology, B-1200 Bruxelles, Belgium

Submitted August 4, 1999; Revised November 2, 1999; Accepted November 30, 1999
Monitoring Editor: Suzanne R. Pfeffer

It is well established that dynamin is involved in clathrin-dependent endocytosis, but relatively little is known about possible intracellular functions of this GTPase. Using confocal imaging, we found that endogenous dynamin was associated with the plasma membrane, the *trans*-Golgi network, and a perinuclear cluster of cation-independent mannose 6-phosphate receptor (CI-MPR)–containing structures. By electron microscopy (EM), it was shown that these structures were late endosomes and that the endogenous dynamin was preferentially localized to tubulovesicular appendices on these late endosomes. Upon induction of the dominant-negative dynK44A mutant, confocal microscopy demonstrated a redistribution of the CI-MPR in mutant-expressing cells. Quantitative EM analysis of the ratio of CI-MPR to lysosome-associated membrane protein-1 in endosome profiles revealed a higher colocalization of the two markers in dynK44A-expressing cells than in control cells. Western blot analysis showed that dynK44A-expressing cells had an increased cellular procathepsin D content. Finally, EM revealed that in dynK44A-expressing cells, endosomal tubules containing CI-MPR were formed. These results are in contrast to recent reports that dynamin-2 is exclusively associated with endocytic structures at the plasma membrane. They suggest instead that endogenous dynamin also plays an important role in the molecular machinery behind the recycling of the CI-MPR from endosomes to the *trans*-Golgi network, and we propose that dynamin is required for the final scission of vesicles budding from endosome tubules.

INTRODUCTION

The cation-independent mannose 6-phosphate receptor (CI-MPR) transports newly synthesized lysosomal enzymes from the *trans*-Golgi network (TGN) to endosomes, where the acidic pH causes release of the ligand, making the receptor free to recycle to the TGN (Duncan and Kornfeld, 1988; Goda and Pfeffer, 1988). The CI-MPR recycling from endosomes to the TGN seems to be a strictly controlled event. Rab9 is essential for the transport between endosomes and the TGN (Lombardi *et al.*, 1993; Riederer *et al.*, 1994; Diaz *et al.*, 1997), and α-SNAP and NSF stimulate the in vitro transport of CI-MPR from endosomes (Itin *et al.*, 1997). Although budding of clathrin-coated vesicles from endosomes has been reported (Stoorvogel *et al.*, 1996), clathrin does not seem to be required for the transport of CI-MPR from late endosomes to the TGN (Draper *et al.*, 1990; Goda and Pfeffer, 1991) in a reconstituted cell-free system (Goda and Pfeffer, 1988). Recently, a new protein, called TIP47, was found to be important for the endosomal sorting of CI-MPR, probably by acting in cargo selection (Diaz and Pfeffer, 1998). The recruitment of TIP47 is enhanced in the presence of GTPγS, indicating that a GTPase could be involved in the budding step (Diaz and Pfeffer, 1998). The budding step also seems to require ETF-1, an *N*-ethylmaleimide–sensitive factor different from NSF (Goda and Pfeffer, 1991). ETF-1 is needed at an early stage of the formation of recycling vesicles, and it has

† Present address: Consorzio Mario Negri Sud, 66030 S. Maria Imbaro, Italy.
‖ Corresponding author. E-mail address: b.v.deurs@mai.ku.dk.
Abbreviations used: CD-MPR, cation-dependent mannose 6-phosphate receptor; CI-MPR, cation-independent mannose 6-phosphate receptor; EM, electron microscopy; Lamp-1, lysosome-associated membrane protein-1; TGN, *trans*-Golgi network.

been proposed that it participates in the generation of vesicle curvature (budding) and/or in the scission of the budding endosome membrane to form a recycling vesicle (Goda and Pfeffer, 1991).

The GTP-binding protein dynamin appears to be another relevant candidate when searching for molecules involved in the formation of recycling vesicles that mediate transport from endosomes to the TGN. Dynamin is a member of a large protein family involved in membrane fission and vesicular traffic, and it is expressed in a wide variety of organisms (van der Bliek, 1999). In mammals, three dynamin isoforms (and numerous splice variants) exist: dynamin-1, which is specific to neuronal cells; dynamin-2, which is ubiquitously expressed in nonneuronal cells; and dynamin-3, which is expressed in special cell types (from testis, brain, and lung) (Cao *et al.*, 1998). Dynamin is involved in the formation of clathrin-coated endocytic vesicles at the plasma membrane (McNiven, 1998; Schmid *et al.*, 1998). Overexpression of dominant-negative mutants of both dynamin-1 (K44A and K44E) and dynamin-2 (K44A) leads to inhibition of clathrin-dependent endocytosis in nonneuronal cells (Damke *et al.*, 1994; Altschuler *et al.*, 1998; Vickery and von Zastrow, 1999). Overexpression of dynK44A in HeLa cells does not affect the clathrin-independent endocytosis of the plant toxin ricin but impairs its intracellular trafficking (Llorente *et al.*, 1998). Dominant-negative dynamin decreases ricin accessibility to the TGN, as assessed by ultrastructural tracking of a ricin-peroxidase conjugate and by measuring sulfation of a modified ricin containing a sulfation site. Moreover, it impairs cell intoxication, which depends on retrograde transport of ricin from endosomes to the TGN/Golgi complex and from there to the endoplasmic reticulum (Llorente *et al.*, 1998). Dynamin has been localized at the TGN, and its involvement in the budding of clathrin-coated and other vesicles from the TGN has been reported (Henley and McNiven, 1996; Maier *et al.*, 1996; Jones *et al.*, 1998). However, with the exception of the above-mentioned ricin work, no studies to date have reported any functional association of dynamin with endosomes, and a role of dynamin in intracellular membrane trafficking has been challenged by two recent reports claiming that dynamin is exclusively associated with the plasma membrane and has no effect on intracellular trafficking (Altschuler *et al.*, 1998; Kasai *et al.*, 1999).

The present study aimed to clarify this controversy by addressing two related questions. Structurally, is endogenous dynamin associated with intracellular structures involved in endosome-to-TGN recycling of the CI-MPR? Functionally, is not only endosome-to-TGN transport of ricin but also that of an endogenous protein such as the CI-MPR affected by overexpression of dynK44A? We combined confocal microscopy and electron microscopy (EM) and found that 1) endogenous dynamin localizes intracellularly to CI-MPR–containing endosomes, in particular to CI-MPR–containing tubulo-vesicular components of these endosomes; and 2) overexpression of mutant dynamin leads to endosome tubulation and a downstream redistribution of the CI-MPR from endosomes to prelysosomal structures. Together, these results suggest that dynamin is part of the molecular machinery involved in the vesiculation of endosome tubules required for CI-MPR recycling.

MATERIALS AND METHODS

Cell Culture

HeLa dynK44A cells were kindly provided by Dr. S.L. Schmid (The Scripps Research Institute, La Jolla, CA). The cells were grown in Nunc T75 flasks and maintained in DMEM supplemented with 10% FCS, 100 U/ml penicillin, 100 μg/ml streptomycin, 2 mM L-glutamine, 400 μg/ml geneticin, 200 ng/ml puromycin, and 1 μg/ml tetracycline (from a stock of 1 mg/ml in ethanol) (Damke *et al.*, 1994, 1995a,b). Cells between the 4th and 15th passages were used for experiments. Cells were seeded (2.5×10^5 in T25 flasks or 10^4 in glass chamber slides) (Nalge Nunc, Naperville, IL) and grown in the presence or absence of 1 μg/ml tetracycline for 48 or 72 h. A total of 2 mM butyric acid (Sigma, St. Louis, MO) was added for the last 24 h when the culture time was prolonged to 72 h. Cell viability was tested by trypan blue exclusion.

Transferrin Uptake

Holo-transferrin (Sigma) was iodinated by the iodogen method. Cells were seeded in 24-well plates (1.5×10^4 per well) and grown as described above. Cells were washed twice and incubated for 30 min with HEPES-buffered DMEM/0.2% BSA at 37°C before addition of ^{125}I-transferrin (200 ng/ml). After 5 min at 37°C, the cells were washed in cold DMEM/BSA, and the cell surface–associated ^{125}I-transferrin was removed by ice-cold 100 mM NaCl, 50 mM glycine-HCl, pH 2.8, for 5 min. Internalized ^{125}I-transferrin was extracted by cell lysis with 1 M NaOH. Radioactivity was measured by a γ-counter (1270 rack gamma II, LKB Wallac, Turku, Finland). Intracellular uptake was calculated as internalized counts per minute $\times$ 100/internalized counts per minute + cell surface counts per minute.

Protein Degradation Assay

Inhibition of lysosomal proteolysis was tested after treatment of cells for 24 h with leupeptin (50 μg/ml) and pepstatin (66 μg/ml) (Sigma). Cells were incubated for 2 h at 20°C in the presence of 2 nM ^{125}I-EGF (Amersham-Pharmacia Biotech, Uppsala, Sweden; specific activity, 1306 Ci/mmol; radioactive concentration, 100 μCi/ml). The medium was then replaced with DMEM/HEPES and cells were chased for 4 h at 37°C. Protein was precipitated by adding 10% trichloroacetic acid to the medium on ice for 2 h, followed by centrifugation for 5 min in a table microfuge. Cells were lysed in 1 M NaOH. Radioactivity associated with cell lysates, supernatant fractions, and pellets was measured in a γ-counter.

Western Blotting

Cells were washed twice with PBS (without Ca^{2+} and Mg^{2+}), scraped off, and pelleted. A total of 200 μl of Laemmli buffer (without β-mercaptoethanol) was added to the pellet, and the lysate was stored at −20°C. The protein concentration was determined by the detergent-compatible Bio-Rad (Richmond, CA) colorimetric assay according to the manufacturer. Proteins were resolved as reported (Laemmli, 1970) in 10% or 4–20% SDS-PAGE (Novex, Encinitas, CA) and blotted to a nitrocellulose membrane (Hybond ECL, Amersham Life Science, Arlington Heights, IL). The membrane was incubated for 1 h in blocking solution (10% nonfat dry milk [Bio-Rad], 0.1% Tween 20 [Merck, Rahway, NJ] in PBS).

Dynamin was detected by mouse monoclonal anti-dynamin-1 (hudy-1; kindly provided by Dr. S.L. Schmid) or rabbit polyclonal anti-dynamin-2 (anti-dyn2; kindly provided by Dr. M. McNiven, Mayo Clinic, Rochester, MN). Cathepsin D was detected by rabbit polyclonal anti-cathepsin D (Dako, Carpenteria, CA) in the lysate or by mouse monoclonal anti-cathepsin D (Calbiochem, La Jolla, CA) after immunoprecipitation (see below) from the medium. Development was performed with a chemiluminescent detection kit (ECL, Amersham Life Science). Quantitation of the blotted signal was

performed with the MetaMorph imaging system (Universal Imaging, West Chester, PA).

Immunoprecipitation

Medium from the last 24 h of culture was collected and pelleted. The supernatant was then precleared for 1 h at 4°C with Gammabind Plus Sepharose (Pharmacia Biotech, Piscataway, NJ) and subsequently was incubated overnight at 4°C in the presence of 10 μg/ml rabbit anti-cathepsin D (Dako) and Gammabind Plus Sepharose. After spinning, the pellet was kept at −20°C and Western blotted after lysis in Laemmli buffer.

Immunofluorescence and Confocal Microscopy

Cells grown on glass chamber slides were washed twice with PBS, fixed with 2% formaldehyde in 0.1 M phosphate buffer, pH 7.2, for 1 h, and washed twice with PBS before permeabilization/blocking in 0.2% saponin/5% normal goat serum (in PBS). Then the cells were incubated with various antibody combinations as indicated (30 min at room temperature for each antibody). The antibodies used were hudy-1, anti-dyn2, rabbit anti-human CI-MPR (kindly provided by Dr. K. von Figura, Göttingen University, Göttingen, Germany), and rabbit anti-TGN-38 serum (kindly provided by Dr. M. McNiven). The primary antibodies were detected by goat anti-mouse or anti-rabbit immunoglobulin G coupled to Alexa 568 or Alexa 488 (Molecular Probes, Eugene, OR). Cells were washed three times for 5 min each with permeabilization/blocking buffer between each step of incubation. Actin was detected by FITC-conjugated phalloidin (Sigma). Coverslips were mounted with the ProLong antifade kit (Molecular Probes), and the specimens were analyzed with a Zeiss (Thornwood, NY) LSM 510 confocal microscope equipped with Ar (458 and 488 nm) and HeNe (543 nm) lasers. The objective lens used was a c-Apochromat 63×/1.2 Water corr.; the image size was 1024 × 1024 pixels (8-bit pixel depth), and the pinhole setting was 100 (corresponding to 0.81 Airy units).

Analytical Subcellular Fractionation

Cells (~4×10^7) were washed twice with PBS and once with ice-cold 250 mM sucrose buffered with 3 mM imidazole-HCl, pH 7.4. Cells were scraped off and homogenized in the buffered sucrose solution with a Dounce homogenizer (piston tight B). After nuclei and cell debris were removed at 8700 $g \times$ min (E4 rotor, GR4.11, Société Jouan-Saint Herblain, France; N fraction), postnuclear particles were pelleted at 6×10^6 $g \times$ min (Ti50 rotor, Beckman, Fullerton, CA). This fraction was layered over a linear gradient (1.10–1.30 g/ml) for isopycnic centrifugation (48×10^6 $g \times$ min; SW40 rotor, Beckman). Twenty fractions of ~500 μl each were collected, weighed, and analyzed for density, enzyme activities, and antigenic content by quantitative Western blotting. Proteins, alkaline phosphodiesterase, and lysosomal enzyme activities were determined with the use of established procedures (Cornillie *et al.*, 1991; Courtoy, 1993). Except for CI-MPR (which gave a weak signal), recoveries in gradients ranged between 80 and 125%.

Equal volumes of each gradient fraction were boiled for 3 min in SDS-PAGE sample buffer containing 0.1 M DTT (for lysosome-associated membrane protein-1 [Lamp-1]) or not (for CI-MPR) and resolved on 5–10% gradient SDS-polyacrylamide gels. Proteins were transferred from the gel to a polyvinylidene difluoride membrane during 16 h at 250 mA in 100 mM Tris, 16 mM glycine, and 20% methanol. Western blotting was performed with the use of a 1:200 dilution of the above-mentioned rabbit antiserum against CI-MPR (see Immunofluorescence and Confocal Microscopy) or a 1:2500 dilution of rabbit anti-human Lamp-1 antiserum (kindly provided by Dr. Sven Carlsson, Umeå University, Umeå, Sweden), both for 16 h at 4°C. All washing steps were made with 2% (wt/vol) BSA in the same buffer. Bound antibodies were detected with ^{125}I-protein A (30 mCi/mg, 1 μCi/blot, Amersham) for 5 h at room temperature. Polyvinylidene difluoride membranes were exposed for 48 h to a phosphor screen, read, and quantified by Phosphoimager (Molecular Dynamics, Sunnyvale, CA). Distributions in the gradients were finally standardized into 20 ideal fractions with equal density intervals, and activity of the different constituents was reported as frequency (Courtoy, 1993).

Electron Microscopy

Cells were washed twice in PBS and fixed for 1 h at room temperature with 0.1% glutaraldehyde and 2% formaldehyde in 0.1 M phosphate buffer, pH 7.2. In some experiments, the cells were incubated at 37°C for 90 min with cationized gold (20 nm) or for 2 h followed by a 2-h chase with BSA-gold (5 nm) (both from British BioCell International, Cardiff, United Kingdom) before fixation. Before the gold markers were used for internalization experiments, they were dialyzed overnight against DMEM/HEPES in Spectra/Por molecular porous membrane tubes (molecular weight cutoff 12–14000, Spectrum Medical Industries, Houston, TX) and diluted 1:8. After fixation, cells were scraped off, sedimented for 30 min at room temperature, spun for 1 min in a microfuge, and then embedded in 7.5% gelatin (Merck) in PBS for 30 min at 37°C. After cooling on ice and trimming, cell pellets were infused twice for 30 min each with 2.1 and 2.3 M sucrose, respectively, mounted on aluminum stubs, and frozen in liquid nitrogen. Ultrathin sections were cut by a Reichert (Vienna, Austria) Ultracut S microtome, collected with 2.3 M sucrose, and mounted on Formvar-coated copper or nickel grids.

Detection of CI-MPR and Lamp-1 was performed with the above-mentioned anti-CI-MPR antiserum (see Immunofluorescence and Confocal Microscopy) and anti-human Lamp-1 antiserum (see Analytical Subcellular Fractionation), followed by protein A-gold (Slot and Geuze, 1984). Protein A-gold (10- and 15-nm gold) was purchased from Dr. G. Posthuma (Utrecht University, Utrecht, The Netherlands). Dynamin was detected with hudy-1 followed by gold-conjugated goat anti-mouse immunoglobulin G (5 nm; Amersham Life Technologies).

In some experiments, cells internalized HRP (Sigma type II), 5 mg/ml in DMEM/HEPES, for 30 or 50 min at 37°C before fixation in 0.5% glutaraldehyde and 4% formaldehyde in 0.1 M phosphate buffer, pH 7.2. After washing in PBS, the fixed cells were incubated for 60 min at room temperature with PBS containing 0.5 mg/ml diaminobenzidine and 0.5 μl of 30% H_2O_2/ml, washed, and processed for Epon embedding. Finally, in some experiments, cells were incubated with cationized gold or BSA-gold as described above before fixation with 2% glutaraldehyde in 0.2 M Na-cacodylate buffer, pH 7.4, in the presence of 0.5 mg/ml ruthenium red. The cells were postfixed for 60 min in 2% OsO_4 in 0.2 M Na-cacodylate buffer, pH 7.4, in the presence of 0.5 mg/ml ruthenium red, washed in the same buffer, and embedded in Epon.

Sections were analyzed in a Jeol (Tokyo, Japan) 100 CX or a Philips (Eindhoven, The Netherlands) 100 CM electron microscope.

RESULTS

Localization of Endogenous Dynamin in HeLa Cells

In the first part of this study, we examined whether endogenous dynamin unequivocally localized to intracellular structures of relevance for the recycling of the CI-MPR, by a combination of confocal microscopy and immunogold labeling EM.

For the detection of dynamin-2 in HeLa cells, two different antibodies were tested: a polyclonal antibody against a conserved region of the various dynamin-2 splice variants (anti-dyn2) and a mAb detecting both dynamin-1 and dynamin-2 (hudy-1). Both antibodies revealed a distinct ~100-kDa band on Western blots of HeLa cell lysates. In confocal images, both antibodies gave a specific, punctate labeling in HeLa

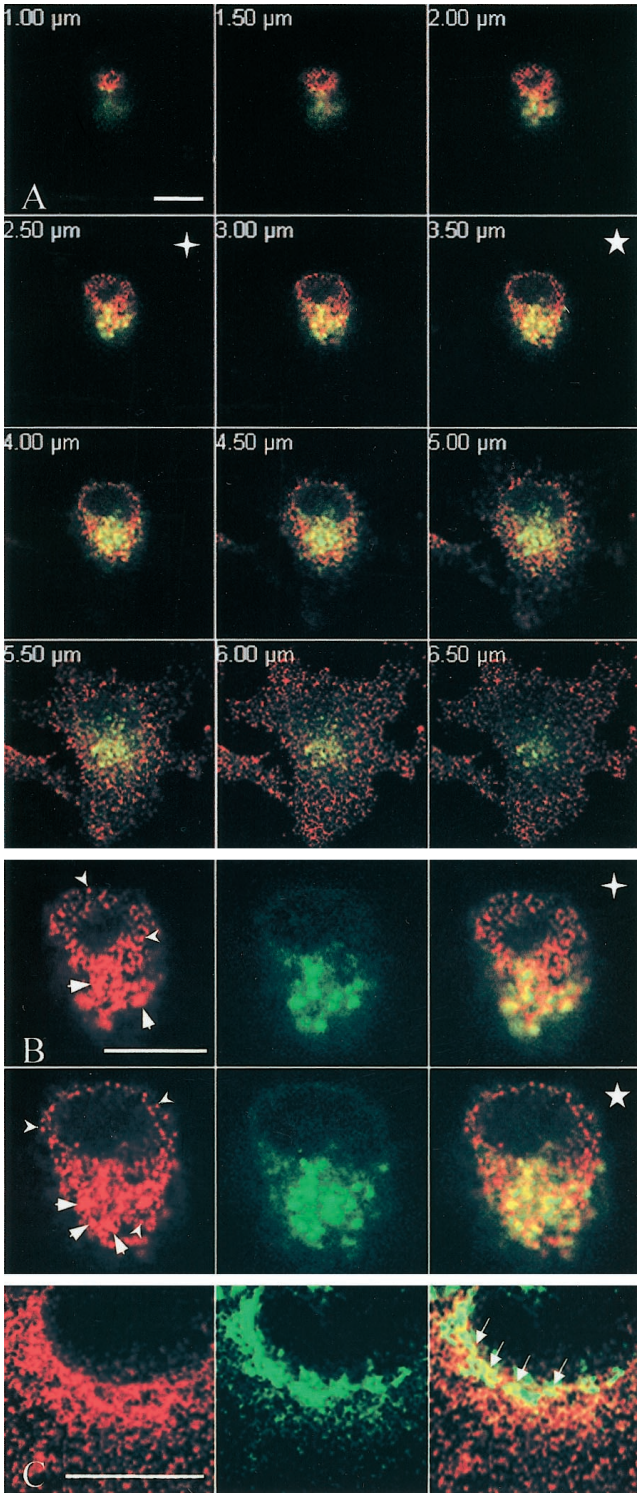

Figure 1. Distribution of endogenous dynamin in HeLa cells. HeLa dynK44A cells grown in the presence of tetracycline were fixed, permeabilized, and double labeled for dynamin (red in A–C) and CI-MPR (green in A and B) or for dynamin and TGN-38 (green in C). (A) Merged images obtained by confocal sectioning from the dorsal top to the ventral surface of a representative cell at 0.5-μm intervals. Note that although the dynamin signal derives in part from the plasma membrane, dynamin distinctly colocalizes with CI-MPR in the perinuclear region (yellow). (B) Split red, green, and merged channels of the 2.5-μm (+) and 3.5-μm (*) confocal section planes at higher magnification. Endogenous dynamin appears as both small dots (arrowheads) and larger, coarse dots (arrows), the latter colocalizing with the CI-MPR. (C) Dynamin also colocalizes to some extent with TGN-38 (arrows in the merged image). Bars, 10 μm.

cells and showed colocalization in double-labeling experiments. Thus, hudy-1 detected the same structural patterns as did anti-dyn2. However, in highly enlarged confocal images, it was evident that the sensitivity and resolution were better with hudy-1 than with anti-dyn2. Moreover, when tested on ultracryosections by immunogold labeling (see below), only hudy-1 gave satisfactory labeling. In all experiments described below, therefore, hudy-1 was used.

When the localization of dynamin-2 was analyzed by confocal sectioning, the punctate signal was obtained all the way through the cell (Figure 1A). A proportion corresponded to the plasma membrane, because it was most distinct on the top of the cells, and particularly when the focal plane was close to the ventral surface. In addition, there was consistent coarse-dotted labeling for dynamin in the perinuclear region. This perinuclear dynamin labeling colocalized to a large extent with the CI-MPR (Figure 1B) and with the late endosome/lysosome marker Lamp-1 (CI-MPR and Lamp-1 also showed some degree of colocalization; see below), confirming that the labeling was indeed intracellular. Furthermore, some of the perinuclear dynamin labeling clearly colocalized with TGN-38 (Figure 1C), as reported previously for other cell types (Cao *et al.*, 1998).

However, although confocal microscopy offers many advantages, the limited structural resolution obtained by immunofluorescence may complicate the interpretation of the images, particularly when studying membrane traffic (Griffiths *et al.*, 1993). Therefore, to provide a precise identification of the intracellular structures associated with endogenous dynamin, immunogold labeling of ultracryosections was analyzed by EM. As shown in Figure 2A, hudy-1 detected dynamin-2 on clathrin-coated pits at the plasma membrane, as reported previously (Damke *et al.*, 1994). The TGN and associated clathrin-coated structures were also consistently labeled for dynamin (Figure 2B), thus confirming the confocal results. Most importantly, however, endosomes and in particular tubulo-vesicular structures connected with or localized close to the endosomes were distinctly labeled for dynamin (Figure 2, C–F). These endosomes, which often appeared as multivesicular bodies, contained internalized BSA-gold or cationized gold and were distinctly labeled for the CI-MPR. It has been shown that in HeLa cells the CI-MPR is almost exclusively localized to late endosomes rather than to the TGN (Mallard *et al.*, 1998). Thus, it is justified to conclude that the dynamin-associated, CI-MPR–containing endosomes reported here are indeed late endosomes. In general, the tubulo-vesicular structures did not appear to be clathrin coated. A quantitative analysis of the cellular distribution of dynamin is shown in Figure 3. Moreover, quantification revealed that 85% of the late endosome–associated dynamin was bound to the tubulo-vesicular component, whereas 15% was present on the vacuolar component of the CI-MPR–containing endosomes.

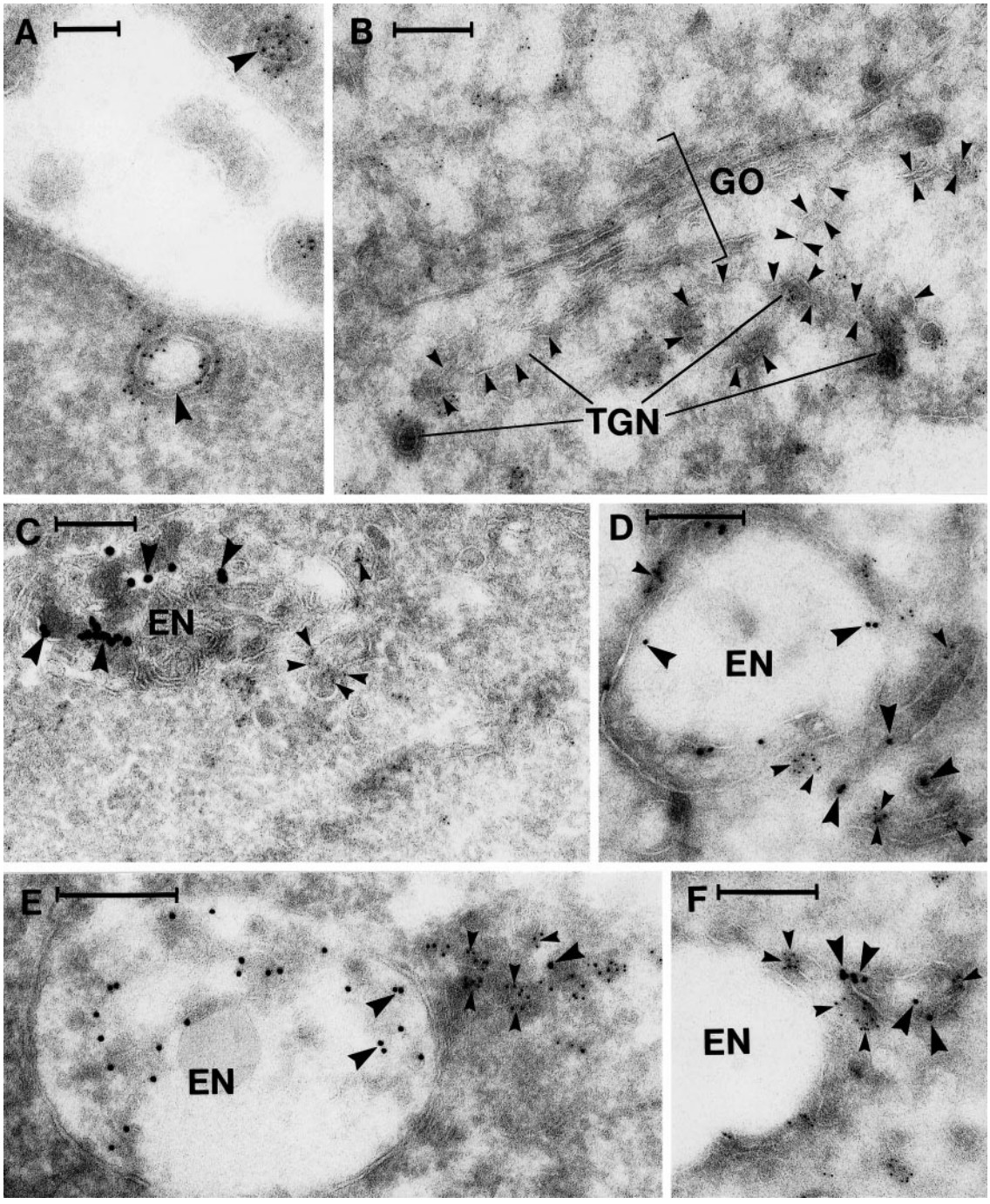

Figure 2. Localization of endogenous dynamin by immunogold labeling of ultracryosections. The localization of endogenous dynamin in HeLa dynK44A cells grown in the presence of tetracycline was determined by labeling of ultracryosections with the hudy-1 antibody (5-nm gold). Dynamin is localized to clathrin-coated pits at the cell surface (large arrowheads in A) and to the TGN adjacent to a Golgi stack (GO in B), where the membrane network characteristic of the TGN is outlined by arrowheads. Moreover, dynamin is localized to endosomes (EN) that contain internalized 20-nm cationized gold particles (large arrowheads in C) and CI-MPR (10-nm gold; large arrowheads in D–F). Note that dynamin (small arrowheads in C–F) is localized mainly to tubulo-vesicular extensions of the endosomes. Bar in A, 100 nm; bars in B–F, 200 nm.

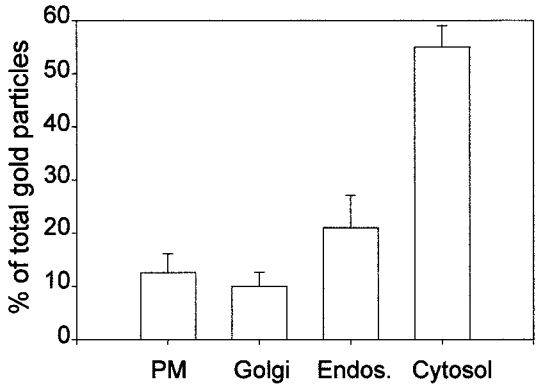

Figure 3. Relative distribution of endogenous dynamin between the plasma membrane and the intracellular compartments. Ultracryosections from three different HeLa dynK44A cultures (at least two passages apart) grown in the presence of tetracycline were labeled with the hudy-1 antibody. Gold particles (5 nm) associated with or <100 nm away from the plasma membrane, including clathrin-coated pits (PM), Golgi stacks/TGN (Golgi), vacuolar and tubulo-vesicular endosomes (Endos.), and the cytosol, including unidentified cytosolic objects (Cytosol), were counted on randomly photographed EM pictures (magnification, ×84,000). A total of 8018 gold particles were scored. Values are means ± SE (n = 3).

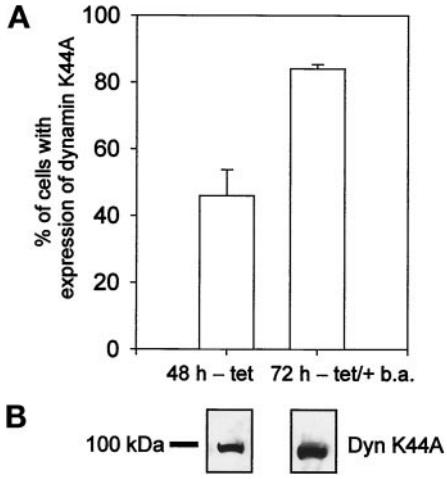

Figure 4. Enhancement of mutant dynamin expression. (A) HeLa dynK44A cells were grown for 48 h without tetracycline (−tet) or for 72 h without tetracycline and in the presence of the transcriptional activator butyric acid (2 mM) for the last 24 h (−tet/+b.a.). The cells were then fixed, and double fluorescence labeling for dynamin (with the use of hudy-1) and actin was performed to determine the frequency of cells positive for mutant dynamin relative to cells positive for actin, which is present in all cells (mean ± SE, n = 3). (B) Representative Western blot of dynamin expression in HeLa dynK44A cells grown under the conditions described in A.

Enhancement of the Frequency of dynK44A-expressing HeLa Cells

Having established that endogenous dynamin is concentrated on tubulo-vesicular processes of CI-MPR–containing endosomes in HeLa cells, we tested its function by overexpressing the dominant-negative dynamin-1 mutant dynK44A in the same cells. Because this analysis is based partly on quantitative EM (see below), in which randomly chosen endosomes are studied in sections through a pellet made by scraping off cells from the culture flask, we aimed to maximize the frequency of dynK44A-expressing cells in the cultures. Accordingly, expression of dynK44A was tested by immunofluorescence and Western blot analyses at different times of culture (48 or 72 h) with or without tetracycline and in the presence or absence of a transcriptional enhancer (2 mM butyric acid for the last 24 h). The percentage of cells overexpressing dynK44A was first determined by double fluorescence labeling with the use of actin as a general marker of all cells in culture. As shown in Figure 4A, after 48 h without tetracycline and butyric acid, <50% of the cells showed a high expression of dynK44A, but this proportion increased to 80% when cells were incubated for an additional 24 h without tetracycline and in the presence of butyric acid. In addition, total dynamin content in the lysate was increased 1.8 ± 0.2-fold (mean ± SE, n = 4) by this procedure (referred to hereafter as "enhanced K44A expression") (Figure 4B).

Cell viability was not affected by the culture condition for enhanced expression of mutant dynamin (<1% staining with trypan blue in both conditions). Moreover, we found no effect of the additional incubation with butyric acid on the abundance of the transferrin receptor, CI-MPR, and Lamp-1 or on the enzyme activity of cathepsin D, *N*-acetyl-β-hexosaminidase, acid phosphatase, acid mannosidase, and acid fucosidase (our unpublished results). Therefore, both protocols were used for the confocal studies reported below, and the protocol for enhanced dynK44A expression was selected for the quantitative EM.

Expression of dynK44A Causes Redistribution of CI-MPR

To elucidate the possible function of dynamin on CI-MPR–containing vacuolar endosomes and in particular on their tubulo-vesicular appendices, dynK44A was expressed in the HeLa cells. Both after 48 h of culture without tetracycline and after the protocol for enhanced K44A expression, overexpression of dynK44A strongly reduced transferrin uptake (Figure 5), as reported previously after incubation for 48 h without tetracycline (Damke *et al.*, 1994; Llorente *et al.*, 1998).

In the confocal microscope, cells overexpressing mutant dynamin presented such an intense fluorescence signal that no distinct cytoplasmic structures were distinguishable (Figure 6A, C, and E, large arrows). In contrast, adjacent cells without detectable overexpression of mutant dynamin showed the typical punctate staining for endogenous dynamin described above. When cultures were double labeled for dynamin and CI-MPR, a characteristic change in the localization of CI-MPR was consistently observed in the cells overexpressing mutant dynamin, regardless of the dynK44A induction protocol used. In overexpressing cells, the CI-MPR signal was more dispersed and hence became distinctly dotted (Figure 6, B, D, and F, large arrows) compared with the clustered and thus less distinct appearance in the perinuclear region of control cells (Figure 6, B, D, and F, small arrows).

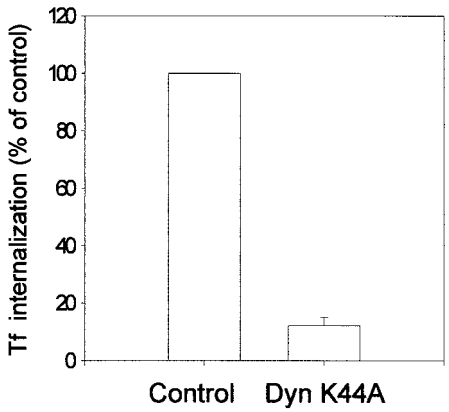

Figure 5. Expression of mutant dynamin inhibits endocytosis of transferrin. HeLa dynK44A cells were grown for 72 h with (Control) or without (Dyn K44A) tetracycline, in both cases in the presence of butyric acid for the last 24 h, and internalization of ^{125}I-transferrin (Tf) was measured (mean ± SE, n = 3).

Ultrastructural Analysis of CI-MPR/Lamp-1 Colocalization

To characterize the compartment to which CI-MPR relocalizes upon expression of mutant dynamin, immunogold labeling of ultracryosections was used and the CI-MPR distribution was quantified in randomly taken pictures. To avoid underestimating the redistribution of the CI-MPR, the proportion of cells expressing dominant-negative dynamin was maximized by taking advantage of the enhanced dynK44A expression procedure (see above).

Because the various markers of the endocytic pathway overlap and the ultrastructure of its different compartments is similar or overlapping (van Deurs *et al.*, 1993, 1996), it is difficult to make any sharp distinction between late endosomes and lysosomes by single labeling. In agreement with this, it was not possible to distinguish between these compartments in sections labeled only for CI-MPR, so no immediate difference between control cells and mutant dynamin–expressing cells was noticed. In both cases, almost all CI-MPR in HeLa cells was intracellular, and the great majority (>90%) was localized to "typical" endosomes (average of 8.9 gold particles per endosome profile, based on quantification of 1414 endosome profiles), whereas labeling of TGN/Golgi structures was very low (fewer than 2 gold particles per TGN/Golgi profile), in agreement with a previous study (Mallard *et al.*, 1998).

Therefore, CI-MPR localization was compared with that of Lamp-1 by double immunogold labeling. Generally, a structure labeled for CI-MPR but not for Lamp-1 is accepted as an endosome, and a structure labeled for Lamp-1 but not for CI-MPR is accepted as a lysosome (Geuze *et al.*, 1988; Griffiths *et al.*, 1988). To classify the intermediate structures, we performed a quantitative analysis of the relative amount of CI-MPR and Lamp-1 labeling in endocytic compartments and used an arbitrary classification based on the extent of colocalization in each profile: type 1, MPR+/Lamp-1− ("classic" endosomes); type 2, MPR/Lamp-1 3:1; type 3, MPR/Lamp-1 2:1; type 4, MPR/Lamp-1 1:2; type 5, MPR/Lamp-1 1:3; type 6, MPR−/Lamp-1+ ("classic" lysosomes) (Figure 7).

Figure 8A shows the frequency of these labeled profiles and the CI-MPR steady-state distribution in the control cells. The most abundant CI-MPR–labeled profiles (~70%) were totally or largely devoid of Lamp-1, and most of the CI-MPR that colocalized with Lamp-1 did so in the type 2 profiles (minimal Lamp-1 content). Under normal (control) conditions, CI-MPR should be sorted and removed efficiently from the endocytic pathway. Both the organelle frequency and the CI-MPR distribution shown in Figure 8A followed this prediction, and in particular a very low frequency of type 4 and type 5 profiles with a small content of CI-MPR was observed. After overexpression of mutant dynamin (Figure 8B), there was a shift of the profiles to more extensive codistribution of CI-MPR with Lamp-1, most of the CI-MPR being colocalized with Lamp-1 in the intermediate type 3 and type 4 profiles. This suggests that the CI-MPR continued to move downstream along the endocytic pathway in these cells. In contrast, the frequency of type 6 profiles (classic lysosomes) was not significantly different in control cells and mutant dynamin–expressing cells (Figure 8), and the total amount of Lamp-1–associated gold particles in the population of type 6 profiles was unchanged (10 and 11% in control type 6 and dynK44A type 6, respectively). Moreover, there was no decrease in type 6 profile frequency after inhibition of lysosomal proteases by the addition of leupeptin and pepstatin for the last 24 h of incubation, confirming that the reason for the unchanged frequency of type 6 profiles in dynK44A-expressing cells was not missorting and degradation of CI-MPR in the lysosomes. Control experiments revealed that leupeptin/pepstatin reduced lysosomal protein degradation by 75%.

The distribution of Lamp-1 was also compared by subcellular fractionation in control cells and cells overexpressing mutant dynamin with the use of linear sucrose density gradients and quantitative Western blotting. Lamp-1 codistributed with hexosaminidase, and their density distributions were not appreciably affected by expression of dominant-negative dynamin (median densities were 1.163 g/ml for Lamp-1 and 1.169 g/ml for hexosaminidase in control cells versus 1.166 and 1.172 g/ml in dominant-negative cells). This is in agreement with the above-mentioned data and suggests that expression of mutant dynamin does not interfere with the delivery of Lamp-1 to lysosomes. Unfortunately, the distribution of CI-MPR in the sucrose gradients could not be resolved from Lamp-1/hexosaminidase–containing lysosomes in either control or dominant-negative HeLa cells.

Cathepsin D Processing in Cells Expressing dynK44A

Human cathepsin D, a lysosomal enzyme transported by the CI-MPR and the cation-dependent mannose 6-phosphate receptor (CD-MPR), is synthesized as a 49-kDa inactive precursor. Upon delivery to an endosomal compartment, it is converted into a single-chain intermediate form of 46 kDa, which is finally processed in lysosomes into a double-chain mature form of 32 and 14 kDa (Gieselmann *et al.*, 1983; Damke *et al.*, 1994). It has been reported that expression of mutant Rab9 causes specific impairment of late endosome-to-TGN transport of CI-MPR (Riederer *et al.*, 1994), leading to a compensatory induction of lysosomal enzymes. In particular, the rate of cathepsin D processing was found to be

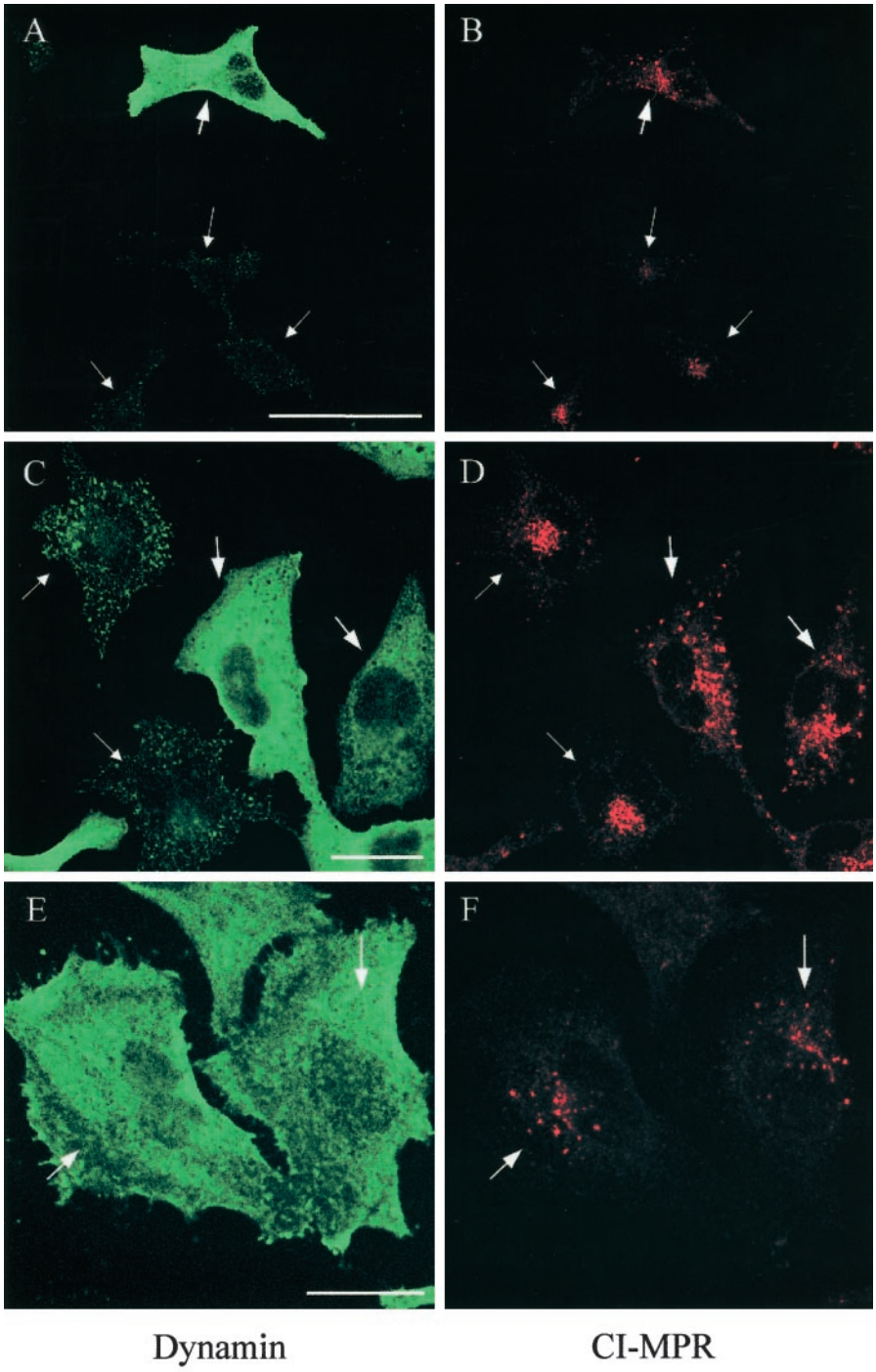

Figure 6. Expression of mutant dynamin causes redistribution of CI-MPR. HeLa dynK44A cells were grown without tetracycline for 48 h (A–D) or without tetracycline for 72 h and with butyric acid added for the last 24 h (E and F) and double-labeled for dynamin (green) and CI-MPR (red). Note that in the mutant dynamin–expressing cells (large arrows), the CI-MPR signal derives from more distinct and widespread structures than in cells without mutant expression (small arrows). The settings of the confocal microscope were adjusted individually in the two channels to make an optimal distinction between endogenous dynamin and mutant dynamin in each image, as well as an optimal CI-MPR signal. Bar in A, 50 μm; bars in C and E, 20 μm.

more than threefold lower than in control cells, resulting in accumulation of the precursor form. Therefore, we analyzed the maturation of cathepsin D in the dynK44A-expressing HeLa cells to test whether the redistribution of the CI-MPR caused by mutant dynamin would also affect lysosomal enzymes. A higher level of procathepsin D (49 kDa) was consistently detected in the cell lysate from mutant dynamin–expressing cells compared with control cells (Figure 9). There was an average twofold increase in procathepsin D content over the control after incubation without tetracycline for 48 h (mean, 230%; range, 170–360%; $n = 3$; $p < 0.05$ by paired *t* tests) and a fourfold increase after the enhanced K44A expression procedure (mean, 389%; range, 141–913%; $n = 6$; $p < 0.05$) (see also Figure 9B). The difference between

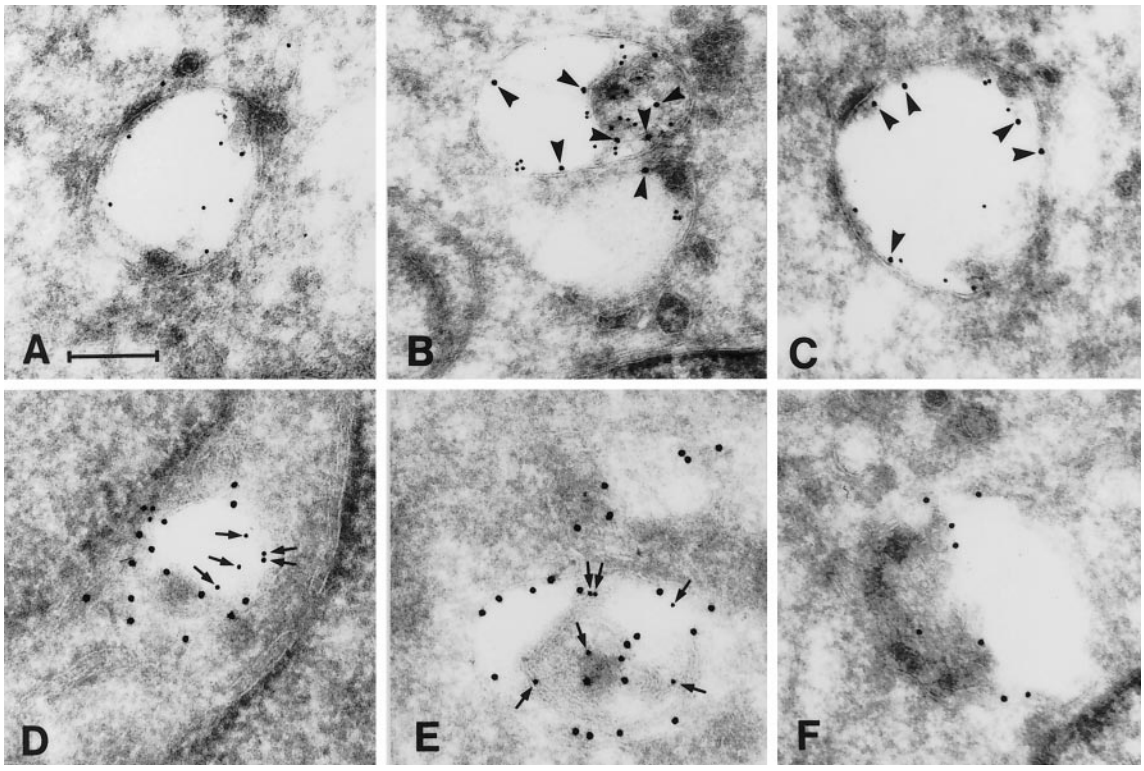

Figure 7. Representative electron micrographs of the patterns of MPR/Lamp-1 distribution as revealed by immunogold double labeling of ultracryosections. Based on the relative amount of gold labeling for CI-MPR and Lamp-1, endocytic structures were grouped into six types (type 1, MPR+/Lamp-1−; type 2, MPR/Lamp-1 3:1; type 3, MPR/Lamp-1 2:1; type 4, MPR/Lamp-1 1:2; type 5, MPR/Lamp-1 1:3; type 6, MPR−/Lamp-1+). Type 1 (only CI-MPR labeling) represents a classic endosome and type 6 (only Lamp-1 labeling) represents a classic lysosome. A–F show examples of types 1–6, respectively. CI-MPR was detected with 10-nm gold (small arrows in D–F), and Lamp-1 was detected with 15-nm gold (arrowheads in A–C). Bar, 200 nm.

the 48- and 72-h incubations parallels the increase in the number of dynK44A-overexpressing cells observed when shifting from one culture condition to the other (see above). In contrast, the abundance of the 32-kDa mature form of cathepsin D was not significantly changed in cells expressing mutant dynamin. Also, no difference in the level of secretion of procathepsin D and the mature form of cathepsin D was detected (Figure 9A).

Expression of dynK44A Increases Endosome Tubulation

To examine whether the above-reported changes in CI-MPR distribution and cathepsin D processing after expression of dynK44A were related directly to structural changes of the endosome compartment, we used EM analysis. With HRP as a general endocytosis marker, we found that the labeling and morphology of endosomes/lysosomes in HeLa cells grown with or without tetracycline were largely the same, but expression of dynK44A often increased endosome tubulation (Figure 10, A–E). The tubulated endocytic compartment was accessible to internalized BSA-gold and cationized gold, and fixation in the presence of ruthenium red allowed us to exclude any connection of the tubules with the cell surface (our unpublished results). In ultracryosections of dynK44A-expressing cells, the endosome tubules were labeled for CI-MPR, whereas dynamin labeling was found associated with these tubules as well as over the cytoplasm (Figure 10, F and G).

DISCUSSION

The data presented here show that endogenous dynamin-2 associates with CI-MPR–containing endosomes, being particularly concentrated on their tubulo-vesicular processes, and that dominant-negative dynamin causes some endosome tubulation and a downstream movement of CI-MPR from these endosomes to a Lamp-1–enriched, prelysosomal compartment. Thus, these results are in contrast to recent studies emphasizing that dynamin-2 is localized exclusively at the plasma membrane and is only involved in formation of clathrin-coated endocytic vesicles (Altschuler *et al.*, 1998; Kasai *et al.*, 1999). Our results suggest instead that endogenous dynamin also could be involved in the recycling of CI-MPR from endosomes to the TGN, presumably by playing an essential role in the generation of recycling vesicles from tubular processes of endosomes. These conclusions are in agreement with other studies indicating that dynamins are involved not only in clathrin-dependent endocytosis but

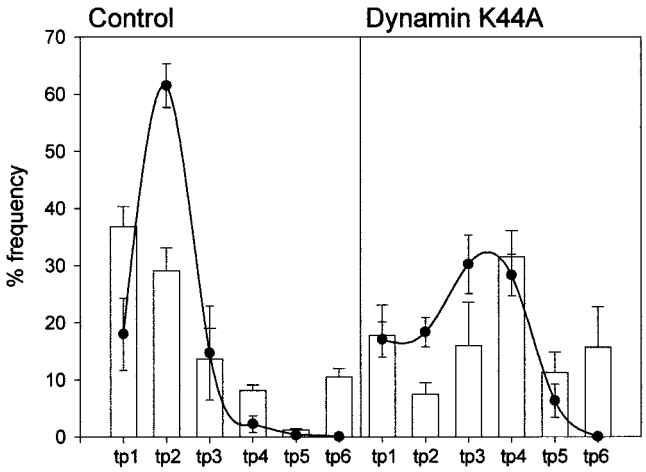

Figure 8. Expression of mutant dynamin causes a redistribution of the CI-MPR to an endocytic compartment strongly positive for Lamp-1 but distinct from classic lysosomes. The frequency of types 1–6 endocytic structures in control cells and cells expressing mutant dynamin was compared based on immunogold double-labeling experiments and the extent of CI-MPR/Lamp-1 colocalization, as described in Figure 7 (bars, mean ± SE, n = 3). Black dots represent the distribution of CI-MPR among the compartments (mean ± SE, n = 3). The material analyzed includes 800 endocytic organelle profiles pooled from three independent experiments with control cells and 614 endocytic organelle profiles from three independent experiments with cells expressing mutant dynamin.

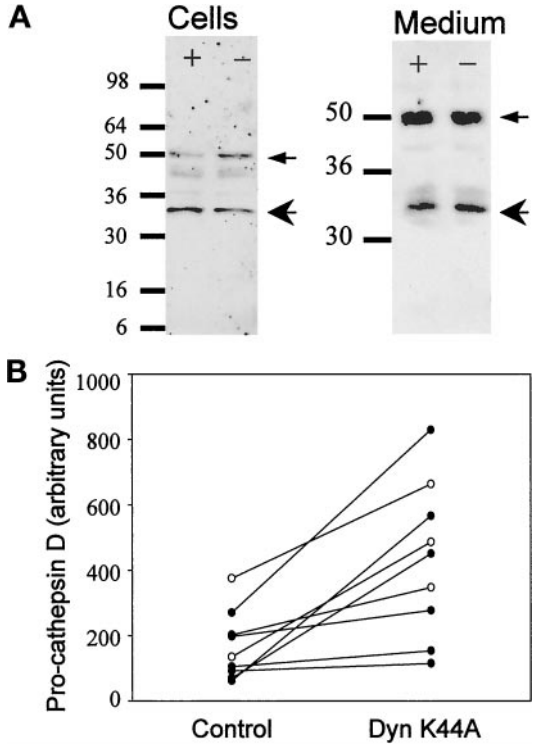

Figure 9. Cathepsin D maturation is perturbed by expression of mutant dynamin. (A) Expression of the lysosomal enzyme cathepsin D (32 kDa) and its precursor procathepsin D (49 kDa) was analyzed by Western blotting of cell lysates (5% of total lysates) and of medium collected from the last 24 h of culture (immunoprecipitates from 50% of medium). When cells were grown without tetracycline (−) in the medium for 48 h, there was a clear increase in cell-associated procathepsin D (left panel). However, even after 72 h without tetracycline and in the presence of butyric acid for the last 24 h, no change was found in the amount of secreted cathepsin into the medium (right panel). Small arrows, procathepsin D; large arrows, mature cathepsin. (B) Graph illustrating the increase in cellular procathepsin D caused by dynK44A expression. The graph is based on scanned blots from three experiments performed after 48 h without tetracycline (○) and six experiments performed after 72 h without tetracycline and in the presence of butyric acid for the last 24 h (●). For a statistical analysis, see text.

also in the transport of ricin from endosomes to the TGN (Llorente *et al.*, 1998), in budding of clathrin-coated and non-clathrin-coated vesicles from the TGN (Henley and McNiven, 1996; Jones *et al.*, 1998), and in vesicle traffic from the endoplasmic reticulum (Yoon *et al.*, 1998). Recently, additional evidence for the involvement of dynamin in intracellular trafficking events came from the observation that productive growth of *Chlamydia* is inhibited in cells expressing dominant-negative dynamin (Boleti *et al.*, 1999).

The CI-MPR redistribution caused by the expression of mutant dynamin was documented by confocal microscopy, whereas the compartment to which the CI-MPR was redistributed was characterized by quantitative EM. To avoid underestimating the change in CI-MPR/Lamp-1 colocalization in dynK44A-overexpressing cells when analyzing random sections through cell pellets, we attempted to maximize the frequency of mutant-expressing cells by improving the induction protocol. Prolonging the incubation without tetracycline to 72 h and adding the transcriptional enhancer butyric acid for the last 24 h increased both the frequency of mutant-expressing cells (from <50% to >80%) and the total expression of mutant dynamin (increased almost twofold as evaluated by Western blotting). These combined data suggest that the average level of dynK44A per expressing cell was essentially the same in the two induction procedures. That the dynamin level does not increase after the first 48 h without tetracycline is in agreement with the reported short half-life of dynamin mRNA and the rapidly reached equilibrium level of the protein after induction (Damke *et al.*, 1995b). Because incubation with the nonspecific transcriptional enhancer butyric acid for the last 24 h could alter the pattern of protein expression, all measurements of dynK44A overexpression except the quantitative EM analysis of CI-MPR/Lamp-1 colocalization have been confirmed after incubation for only 48 h without tetracycline and butyric acid. However, the addition of butyric acid affected neither the abundance of CI-MPR, Lamp-1, and the transferrin receptor nor the activity of several lysosomal enzymes.

The distribution of CI-MPR revealed by the EM quantitation in control HeLa cells reflects the currently accepted model for its recycling (for review, see Hille-Rehfeld, 1995). Most of the CI-MPR localizes in endocytic profiles that are relatively depleted of Lamp-1 (type 2). We believe that this compartment comprises classic late endosomes from which CI-MPR is efficiently transported back to the TGN. In accordance with this, very little CI-MPR was found in types 3–5

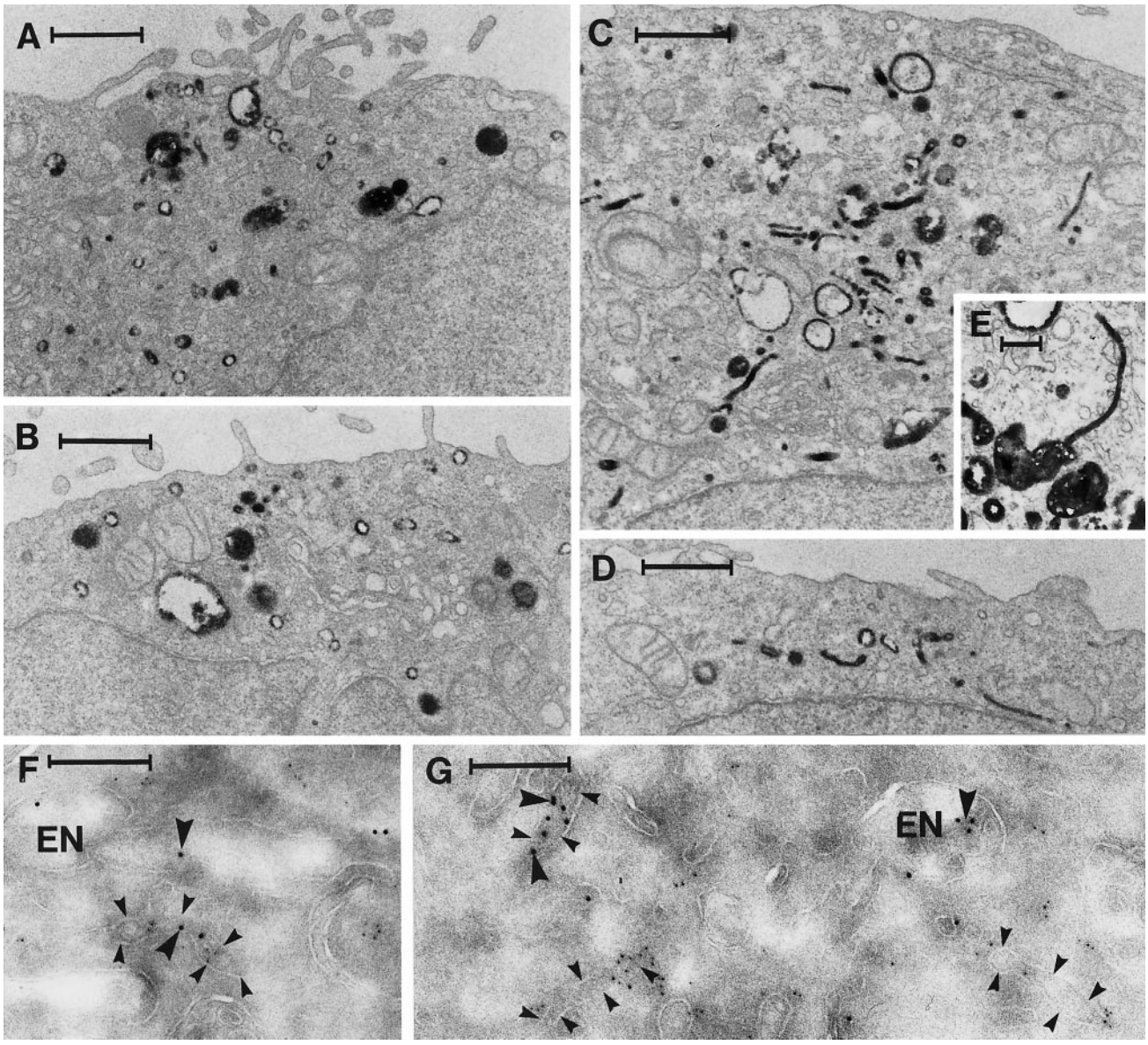

Figure 10. Expression of mutant dynamin causes endosome tubulation. (A and B) HRP-labeled endocytic structures in HeLa dynK44A cells grown in the presence of tetracycline. (C–E) HRP-labeled endocytic structures in the cells grown without tetracycline for 48 h. Cells were incubated with HRP for 30–50 min at 37°C. Note that more tubular endosomes were generated in the mutant-expressing cells. (F and G) Ultracryosections of the tubulated endosomes (small arrowheads) seen in cells expressing dynK44A. The sections were labeled for dynamin (5-nm gold) and CI-MPR (10-nm gold, large arrowheads). Bars in A–D, 1 μm; bars in E–G, 200 nm.

endocytic compartments, which, based on their relative higher content of Lamp-1, are considered to be more mature than classic late endosomes. After induction of mutant dynamin expression, the frequency and CI-MPR content of types 3–5 compartments were both clearly increased, presumably indicating that exit of CI-MPR from the endocytic pathway to the TGN was impaired.

The cytoplasmic tail of the CD-MPR contains a signaling motif that serves to prevent trafficking to lysosomes and to facilitate transport out of endosomes (Rohrer *et al.*, 1995; Schweizer *et al.*, 1996, 1997). When this motif is altered, the mutant receptor is delivered to lysosomes. It has been uncertain, however, whether the CI-MPR would also be missorted to lysosomes when its transport from endosomes to the TGN is impaired. Furthermore, should the CI-MPR still be prevented from moving to lysosomes, would it then accumulate in the (late) endosomes from which recycling to the TGN normally takes place, or would it move downstream to the recently reported prelysosomal hybrid endosome/lysosome compartment (Reaves *et al.*, 1996; Bright *et*

al., 1997; Mullock *et al.*, 1998)? We found that CI-MPR−/Lamp+ (type 6) compartments, which are generally considered to be lysosomes (Geuze *et al.*, 1988; Griffiths *et al.*, 1988), were unaffected after induction of mutant dynamin expression. Our results, therefore, indicate that although the exit of CI-MPR from the endocytic pathway toward the TGN seems to be perturbed by dynK44A overexpression, the CI-MPR is not missorted to lysosomes but accumulates in a prelysosomal compartment. Similarly, Schulze-Garg *et al.* (1993) reported that, after injection of specific antibodies against its cytoplasmic tail, the CD-MPR (the 46-kDa MPR) redistributed to an intermediate compartment on the endocytic pathway in which the receptor segregated from materials destined to lysosomes.

The existence of hybrid prelysosomal organelles has been shown after treatment of cells with wortmannin (Reaves *et al.*, 1996; Bright *et al.*, 1997). Recently, hybrid organelles derived from the fusion of dense lysosomes and endosomes were isolated by cell fractionation (Mullock *et al.*, 1998), and evidence for heterotypic late endosome–lysosome fusions regulated by Rab7 has been obtained (Bucci *et al.*, 2000). The types 3–5 compartment, according to the operational terminology used in the present study, could derive from the fusion of lysosomes and late endosomes (evidence for this was occasionally obtained in our cryosections). Morphological evidence for such fusion has been reported (van Deurs *et al.*, 1995). After expression of mutant dynamin, the fusion would occur between CI-MPR–enriched late endosomes and lysosomes, and the result would be a prelysosomal compartment "contaminated" by CI-MPR.

We also found that the fraction of processed cathepsin D was reduced in cells overexpressing the mutant dynamin, as shown by their increased content of procathepsin D and unchanged level of the mature form. This is similar to results obtained after inhibition of MPR recycling upon mutant Rab9 and mutant Rab7 expression (Riederer *et al.*, 1994; Press *et al.*, 1998). In addition, our results are in agreement with those of Altschuler *et al.* (1998), who observed a delay in cathepsin D processing after expression of either mutant dynamin-1 or mutant dynamin-2 in HeLa cells. The absence of an effect of mutant dynamin on the cellular content of mature 32-kDa cathepsin D is also in agreement with previous observations (Damke *et al.*, 1994). Whereas a detailed analysis of the effects of dominant-negative dynamin on the expression, trafficking, and processing of several lysosomal enzymes is clearly needed, tentative explanations can be offered to account for the increased intracellular content of procathepsin D, the other measured contents being unaffected. First, an unchanged amount of the mature form of cathepsin D in cells that show increased accumulation of procathepsin D, and thus delayed transfer to the maturation compartment, could be due to increased synthesis of procathepsin D or to an increased half-life of the mature enzyme in lysosomes as a consequence of the reduced content of other lysosomal proteases. Second, no increased secretion of either cathepsin D form into the culture medium of mutant dynamin–expressing cells was detected. However, it has been reported that secretion of lysosomal enzymes is mediated by the CD-MPR (Chao *et al.*, 1990), which, in HeLa cells, localizes at steady state mainly to the TGN, in contrast to the CI-MPR, which is concentrated in late endosomes (Mallard *et al.*, 1998; the present study). Overexpression of CD-MPR led to hypersecretion of lysosomal enzymes, which was reversed by microinjection of antibodies against the CD-MPR (Chao *et al.*, 1990). Thus, if expression of mutant dynamin impairs cycling of both MPRs (as would be expected from the present and previous studies [Henley and McNiven, 1996; Jones *et al.*, 1998]), trapping each of them in the major compartments they occupy at steady state, newly synthesized lysosomal proenzymes would preferentially bind to the CD-MPR and stay longer in the TGN and therefore not be secreted.

Although confocal microscopy indicated that endogenous dynamin-2 is associated with an intracellular (perinuclear) CI-MPR–containing compartment, only EM analysis could unequivocally demonstrate this association and reveal the nature of this compartment. This emphasizes that whenever possible, EM should be used to supplement observations made by confocal microscopy. At the EM level, endogenous dynamin was consistently detected on tubulo-vesicular structures close to or connected with CI-MPR–containing endosomes. Whereas the involvement of dynamin in vesicle formation is well established, it remains unclear how this GTPase actually works, whether its effect is direct or indirect, and whether the force applied is constricting or expanding in nature (Kelly, 1999; Kirchhausen, 1999; Sever *et al.*, 1999; Stowell *et al.*, 1999). Because most of the available information on dynamin function derives from cell-free systems, caution is required when extrapolating data to vesiculation in intact cells. Recent in vitro studies on liposomes have shown that dynamin can cause tubulation and subsequent fragmentation or vesiculation of lipid membranes, whereas in the presence of GTPγS, vesiculation is prevented and long tubules are formed (Sweitzer and Hinshaw, 1998; Takei *et al.*, 1998). Tubulation of endosomes as a result of dominant-negative mutant dynamin in intact cells, as reported here, basically agrees with the liposome results and indicates that dynamin participates in vesicle scission. In contrast, our results do not suggest that wild-type dynamin itself causes tubulation in intact cells. Recently, it was reported that amphiphysin-1 is able to generate liposome tubules and to enhance the GTPase and liposome-fragmentation activity of dynamin (Takei *et al.*, 1999). Thus, it could be speculated that endosome tubulation in intact cells is controlled by amphiphysin or amphiphysin-like proteins, whereas dynamin, directly or indirectly by recruiting downstream effectors (Sever *et al.*, 1999), takes care of (recycling) vesicle formation. Dominant-negative dynamin would thereby prevent vesiculation of the nascent tubules and create a shift to long tubular structures. The demonstration that the vast majority of dynamin associated with endosomes is localized to the tubulo-vesicular component rather than to the vacuolar component supports this notion.

The endosome tubulation we observe in the presence of dominant-negative mutant dynamin resembles what has been described previously in cells treated with brefeldin A (Hunziker *et al.*, 1991; Lippincott-Schwartz *et al.*, 1991). This drug inhibits the ARF-coatomer assembly required for vesicle formation (Donaldson *et al.*, 1991; Serafini *et al.*, 1991). However, brefeldin A does not seem to inhibit recycling of the CI-MPR (Chege and Pfeffer, 1990), but another (brefeldin A–insensitive) GTPase may recruit the proteins needed for vesiculation (Diaz and Pfeffer, 1998). It should be noted that we rarely observed clathrin associated with the CI-MPR–

containing endosomes and tubulo-vesicular processes, in agreement with the observation that clathrin is not required for CI-MPR recycling (Draper *et al.*, 1990; Goda and Pfeffer, 1991), whereas TIP47 and ETF-1 could be part of a coat (Goda and Pfeffer, 1991; Diaz and Pfeffer, 1998). In addition to a GTPase–coat protein complex, which may be sufficient for vesicle formation in vitro (Orci *et al.*, 1993; Rothman and Wieland, 1996), dynamin also seems to be required for vesiculation of outgrowing endosome tubules and thereby for CI-MPR recycling in intact cells. Moreover, accumulating data also suggest that the composition of the lipid bilayer, in particular the cholesterol level, may be critical for vesicle formation (Mayor *et al.*, 1998; Mukherjee and Maxfield, 1999; Puri *et al.*, 1999; Rodal *et al.*, 1999). Recently, it was suggested that the retention of cholesterol in late endosomes of Niemann–Pick type C cells (Kobayashi *et al.*, 1999) may lead to membrane changes that perturb the formation of the vesicles involved in recycling from late endosomes to the TGN (Mukherjee and Maxfield, 1999). Therefore, we hypothesize that, provided the endosome membrane has a proper lipid composition, a GTPase–coat protein complex continuously generates vesicular buds from outgrowing endosome tubules, whereas dynamin is responsible for the final scission of these buds and thus for the formation of recycling vesicles.

ACKNOWLEDGMENTS

We are grateful to Ulla Hjortenberg, Mette Ohlsen, Keld Ottosen, and Kirsten Pedersen for excellent technical assistance, to Dr. F. von Bülow for help with the microscopes, and to Dr. Cecilia Bucci for critical comments on the manuscript. This study was supported by grants from the Danish Cancer Society, the Danish Medical Research Council, the John and Birthe Meyer Foundation, the Novo Nordisk Foundation, and the European Community (CT96-0058) to B.v.D.; by grants from the Norwegian Research Council for Science and the Humanities and the Norwegian Cancer Society to K.S.; and by grants from the Novo Nordisk Foundation, the Human Frontier Science Program (RG404/96 M), and the North Atlantic Treaty Organization (collaborative research grant CRG 900517) to B.v.D. and K.S. P.J.C. was supported by the Belgian Fund for Scientific Research. P.N. was working in the van Deurs laboratory with support from the European Community.

REFERENCES

Altschuler, Y., Barbas, S.M., Terlecky, L.J., Tang, K., Hardy, S., Mostov, K.E., and Schmid, S.L. (1998). Redundant and distinct functions for dynamin-1 and dynamin-2 isoforms. J. Cell Biol. *143*, 1871–1881.

Boleti, H., Benmerah, A., Ojcius, D.M., Cerf-Bensussan, N., and Dautry-Varsat, A. (1999). *Chlamydia* infection of epithelial cells expressing dynamin and Eps15 mutants: clathrin-independent entry into cells and dynamin-dependent productive growth. J. Cell Sci. *112*, 1487–1496.

Bright, N.A., Reaves, B.J., Mullock, B.M., and Luzio, P.J. (1997). Dense core lysosomes can fuse with late endosomes and are reformed from the resultant hybrid organelles. J. Cell Sci. *110*, 2027–2040.

Bucci, C., Thomsen, P., Nicoziani, P., McCarthy, J., and van Deurs, B. (2000). Rab7: a key to lysosome biogenesis. Mol. Biol. Cell (*in press*).

Cao, H., Garcia, F., and McNiven, M.A. (1998). Differential distribution of dynamin isoforms in mammalian cells. Mol. Biol. Cell *9*, 2595–2609.

Chao, H.H., Waheed, A., Pohlmann, R., Hille, A., and von Figura, K. (1990). Mannose 6-phosphate receptor dependent secretion of lysosomal enzymes. EMBO J. *9*, 3507–3513.

Chege, N.W., and Pfeffer, S.R. (1990). Compartmentation of the Golgi complex: brefeldin-A distinguishes trans-Golgi cisternae from trans-Golgi network. J. Cell Biol. *111*, 893–899.

Cornillie, F., Brosens, I., Belsey, E.M., Marbaix, E., Baudhuin, P., and Courtoy, P.J. (1991). Lysosomal enzymes in the human endometrium: a biochemical study in untreated and levonorgestrel-treated women. Contraception *43*, 387–400.

Courtoy, P.J. (1993). Analytical subcellular fractionation of endosomal compartments in rat hepatocytes. In: Subcellular Biochemistry, vol. 19, ed. J.J.M. Bergeron and J.R. Harris, New York: Plenum Press, 29–68.

Damke, H., Baba, T., van der Bliek, A, and Schmid, S.L. (1995a). Clathrin-independent pinocytosis is induced in cells overexpressing a temperature-sensitive mutant of dynamin. J. Cell Biol. *131*, 69–80.

Damke, H., Baba, T., Warnock, D.E., and Schmid, S.L. (1994). Induction of mutant dynamin specifically blocks endocytic coated vesicles formation. J. Cell Biol. *127*, 915–934.

Damke, H., Gossen, M., Freundlieb, S., Bujard, H., and Schmid, S.L. (1995b). Tightly regulated and inducible expression of dominant interfering dynamin mutant in stably transformed HeLa cells. Methods Enzymol. *257*, 209–220.

Diaz, E., and Pfeffer, S.R. (1998). TIP47: a cargo selection device for mannose 6-phosphate receptor trafficking. Cell *93*, 433–443.

Diaz, E., Schimmoeller, F., and Pfeffer, S.R. (1997). A novel rab9 effector required for endosome-to-TGN transport. J. Cell Biol. *138*, 283–290.

Donaldson, J.G., Kahn, R.A., Lippincott-Schwartz, J., and Klausner, R.D. (1991). Binding of ARF and β-COP to Golgi membranes: possible regulation by a trimeric G protein. Science *254*, 1197–1199.

Draper, R.K., Goda, Y., Brodsky, F.M., and Pfeffer, S.R. (1990). Antibodies to clathrin inhibit endocytosis but not recycling to the trans-Golgi network in vitro. Science *248*, 1539–1541.

Duncan, J.R., and Kornfeld, S. (1988). Intracellular movement of two mannose 6-phosphate receptors: return to the Golgi apparatus. J. Cell Biol. *106*, 617–628.

Geuze, H.J., Stoorvogel, W., Strous, G.J., Slot, J.W., Bleekemolen, J.E., and Mellman, I. (1988). Sorting of mannose 6-phosphate receptors and lysosomal membrane proteins in endocytic vesicles. J. Cell Biol. *107*, 2491–2501.

Gieselmann, V., Pohlmann, R., Hasilik, A., and von Figura, K. (1983). Biosynthesis and transport of cathepsin D in cultured human fibroblast. J. Cell Biol. *97*, 1–5.

Goda, Y., and Pfeffer, S.R. (1988). Selective recycling of the mannose 6-phosphate/IGF-II receptor to the trans-Golgi network in vitro. Cell *55*, 309–320.

Goda, Y., and Pfeffer, S.R. (1991). Identification of a novel, N-ethylmaleimide-sensitive cytosolic factor required for vesicular transport from endosomes to the trans-Golgi network. J. Cell Biol. *112*, 823–831.

Griffiths, G., Hoflack, B., Simons, K., Mellman, I., and Kornfeld, S. (1988). The mannose 6-phosphate receptor and the biogenesis of lysosomes. Cell *52*, 329–341.

Griffiths, G., Patron, R.G., Lucocq, J., van Deurs, B., Brown, D., Slot, J.W., and Geuze, H.J. (1993). The immuno-fluorescent era of membrane traffic trends. Cell Biol. *3,* 214–219.

Henley, J.R., and McNiven, M.A. (1996). Association of a dynamin-like protein with the Golgi apparatus in mammalian cells. J. Cell Biol. *133*, 761–775.

Hille-Rehfeld, A. (1995). Mannose 6-phosphate receptor in sorting and transport of lysosomal enzymes. Biochim. Biophys. Acta *1241*, 177–194.

Hunziker, W., Whitney, J.A., and Mellman, I. (1991). Selective inhibition of transcytosis by brefeldin A in MDCK cells. Cell *67*, 617–627.

Itin, C., Rancano, C., Nakajima, Y., and Pfeffer, S.R. (1997). A novel assay reveals a role for soluble N-ethylmaleimide-sensitive fusion attachment protein in mannose 6-phosphate receptor transport from endosomes to the trans Golgi network. J. Biol. Chem. *272*, 27737–27744.

Jones, S.M., Howell, K.E., Henley, J.R., Cao, H., and McNiven, M.A. (1998). Role of dynamin in the formation of transport vesicles from the trans-Golgi network. Science *279*, 573–577.

Kasai, K., Shin, H., Shinotsuka, C., Murakami, K., and Nakayama, K. (1999). Dynamin II is involved in endocytosis but not in the formation of transport vesicles from the trans-Golgi network. J. Biochem. *125*, 780–789.

Kelly, R.B. (1999). New twist for dynamin. Nat. Cell Biol. *1*, E8–E9.

Kirchhausen, T. (1999). Cell biology: boa constrictor or rattlesnake? Nature *398*, 470–471.

Kobayashi, T., Beuchat, M.H., Lindsay, M., Frias, S., Palmiter, R.D., Sakuraba, H., Parton, R.G., and Gruenberg, J. (1999). Late endosomal membranes rich in lysobisphosphatidic acid regulate cholesterol transport. Nat. Cell Biol. *1*, 113–118.

Laemmli, U.K. (1970). Cleavage of structural proteins during the assembly of the head of bacteriophage T4. Nature *227*, 680–685.

Lippincott-Schwartz, J., Yuan, L., Tipper, C., Amherdt, M., Orci, L., and Klausner, R.D. (1991). Brefeldin A's effects on endosomes, lysosomes, and the TGN suggest a general mechanism for regulating organelle structure and membrane traffic. Cell *67*, 601–616.

Llorente, A., Rapak, A., Schmid, S.L., van Deurs, B., and Sandvig, K. (1998). Expression of mutant dynamin inhibits toxicity and transport of endocytosed ricin to the Golgi apparatus. J. Cell Biol. *140*, 553–563.

Lombardi, D., Soldati, T., Riederer, M.A., Goda, Y., Zerial, M., and Pfeffer, S.R. (1993). Rab9 functions in transport between late endosomes and the trans Golgi network. EMBO J. *12*, 677–682.

Maier, O., Knoblich, M., and Westermann, P. (1996). Dynamin II binds to the trans-Golgi network. Biochem. Biophys. Res. Commun. *223*, 229–233.

Mallard, F., Antony, C., Tenza, D., Salamero, J., Goud, B., and Johannes, L. (1998). Direct pathway from early/recycling endosomes to the Golgi apparatus revealed through the study of Shiga toxin B-fragment transport. J. Cell Biol. *143*, 973–990.

Mayor, S., Sabharanjak, S., and Maxfield, F.R. (1998). Cholesterol-dependent retention of GPI-anchored proteins in endosomes. EMBO J. *17*, 4626–4638.

McNiven, M.A. (1998). Dynamin: a molecular motor with pinchase action. Cell *94*, 151–154.

Mukherjee, S., and Maxfield, F.R. (1999). Cholesterol: stuck in traffic. Nat. Cell Biol. *1*, E37–E38.

Mullock, B.M., Bright, N.A., Fearon, C.W., Gray, S.R., and Luzio, J.P. (1998). Fusion of lysosomes with late endosomes produces a hybrid organelle of intermediate density and is NSF dependent. J. Cell Biol. *140*, 591–601.

Orci, L., Palmer, D.J., Amherdt, M., and Rothman, J.E. (1993). Coated vesicles assembly in the Golgi requires only coatomer and ARF protein from the cytosol. Nature *364*, 732–734.

Press, B., Feng, Y., Hoflack, B., and Wandinger-Ness, A. (1998). Mutant rab7 causes the accumulation of cathepsin D and cation-independent mannose 6-phosphate receptor in an early endocytic compartment. J. Cell Biol. *140*, 1075–1089.

Puri, V., Watanabe, R., Dominguez, M., Sun, X., Wheatley, C.L., Marks, D.L., and Pagano, R.E. (1999). Cholesterol modulates membrane traffic along the endocytic pathway in sphingolipid-storage diseases. Nat. Cell Biol. *1*, 386–387.

Reaves, B.J., Bright, N.A., Mullock, B.M., and Luzio, J.P. (1996). The effect of wortmannin on the localization of lysosomal type I integral membrane glycoproteins suggests a role for phosphoinositide 3-kinase activity in regulating membrane traffic late in the endocytic pathway. J. Cell Sci. *109*, 749–762.

Riederer, M.A., Soldati, T., Shapiro, A.D., Lin, J., and Pfeffer, S.R. (1994). Lysosome biogenesis requires rab9 function and receptor recycling from endosomes to the trans-Golgi network. J. Cell Biol. *125*, 573–582.

Rodal, S.K., Skretting, G., Garred, Ø., Vilhardt, F., van Deurs, B., and Sandvig, K. (1999). Extraction of cholesterol with methyl-β-cyclodextrin perturbs formation of clathrin-coated endocytic vesicles. Mol. Biol. Cell *10*, 961–974.

Rohrer, J., Schweizer, A., Johnson, K.F., and Kornfeld, S. (1995). A determinant in the cytoplasmic tail of the cation-dependent mannose 6-phosphate receptor prevents trafficking to lysosomes. J. Cell Biol. *130*, 1297–1306.

Rothman, J.E., and Wieland, F.T. (1996). Protein sorting by transport vesicles. Science *272*, 227–234.

Schmid, S.L., McNiven, M.A., and De Camilli, P. (1998). Dynamin and its partners: a progress report. Curr. Opin. Cell Biol. *10*, 504–512.

Schulze-Garg, C., Boker, C., Nadimpalli, S.K., von Figura, K., and Hille-Rehfeld, A. (1993). Tail-specific antibodies that block return of 46,000 M_r mannose 6-phosphate receptor to the trans-Golgi network. J. Cell Biol. *122*, 541–551.

Schweizer, A., Kornfeld, S., and Rohrer, J. (1996). Cysteine^{34} of the cytoplasmic tail of the cation-dependent mannose 6-phosphate receptor is reversibly palmitoylated and required for normal trafficking and lysosomal enzyme sorting. J. Cell Biol. *132*, 577–584.

Schweizer, A., Kornfeld, S., and Rohrer, J. (1997). Proper sorting of the cation-dependent mannose 6-phosphate receptor in endosomes depends on a pair of aromatic amino acids in its cytoplasmic tail. Proc. Natl. Acad. Sci. USA *94*, 14471–14476.

Serafini, T., Orci, L., Amherdt, M., Brunner, M., Kahn, R.A., and Rothman, J.E. (1991). ADP-ribosylation factor is a subunit of the coat of Golgi-derived COP-coated vesicles: a novel role for a GTP-binding protein. Cell *67*, 239–253.

Sever, S., Muhlberg, A.B., and Schmid, S.L. (1999). Impairment of dynamin's GAP domain stimulates receptor-mediated endocytosis. Nature *398*, 481–486.

Slot, J.W., and Geuze, H.J. (1984). Gold markers for single label and double immunolabeling of ultrathin cryosections. In: Immunogold Labeling for Electron Microscopy, ed. J.M. Polak and J.M. Varndell, Amsterdam: Elsevier, 129–142.

Stoorvogel, W., Oorschot, V., and Geuze, H.J. (1996). A novel class of clathrin-coated vesicles budding from endosomes. J. Cell Biol. *132*, 21–33.

Stowell, M.H.B., Marks, B., Wigge, P., and McMahon, H.T. (1999). Nucleotide-dependent conformational changes in dynamin: evidence for a mechanochemical molecular spring. Nat. Cell Biol. *1*, 27–32.

Sweitzer, S.M., and Hinshaw, J.E. (1998). Dynamin undergoes a GTP-dependent conformational change causing vesiculation. Cell *93*, 1021–1029.

Takei, K., Haucke, V., Slepnev, V., Farsad, K., Salazar, M., Chen, H., and De Camilli, P. (1998). Generation of coated intermediates of clathrin-mediated endocytosis on protein-free liposomes. Cell *94*, 131–141.

Takei, K., Slepnev, V.I., Haucke, V., and De Camilli, P. (1999). Functional partnership between amphiphysin and dynamin in clathrin mediated endocytosis. Nat. Cell Biol. *1*, 33–39.

van der Bliek, A.M. (1999). Functional diversity in the dynamin family. Trends Cell Biol. *9*, 96–102.

van Deurs, B., Holm, P.K., Kayser, L., and Sandvig, K. (1995). Delivery to lysosomes in the human carcinoma cell line HEp-2 involves an actin filament-facilitated fusion between mature endosomes and preexisting lysosomes. Eur. J. Cell Biol. *66*, 309–323.

van Deurs, B., Holm, P.K., Kayser, L., Sandvig, K., and Hansen, S.H. (1993). Multivesicular bodies in HEp-2 cells are maturing endosomes. Eur. J. Cell Biol. *61*, 208–224.

van Deurs, B., Holm, P.K., and Sandvig, K. (1996). Inhibition of the vacuolar H^+-ATPase with bafilomycin reduces delivery of internalized molecules from mature multivesicular endosomes to lysosomes in HEp-2 cells. Eur. J. Cell Biol. *69*, 343–350.

Vickery, R.G., and von Zastrow, M. (1999). Distinct dynamin-dependent and -independent mechanisms target structurally homologous dopamine receptors to different endocytic membranes. J. Cell Biol. *144*, 31–43.

Yoon, Y., Pitts, K.R., Dahan, S., and McNiven, M.A. (1998). A novel dynamin-like protein associates with cytoplasmic vesicles and tubules of the endoplasmic reticulum in mammalian cells. J. Cell Biol. *140*, 779–793.